Electron Detachment as a Probe of Intrinsic Nucleobase Dynamics in Dianion–Nucleobase Clusters: Photoelectron Spectroscopy of the Platinum II Cyanide Dianion Bound to Uracil, Thymi…

ARTICLE *in* THE JOURNAL OF PHYSICAL CHEMISTRY B · AUGUST 2015

Impact Factor: 3.3 · DOI: 10.1021/acs.jpcb.5b07108 · Source: PubMed

4 AUTHORS:

Ananya Sen

Argonne National Laboratory

14 PUBLICATIONS **72** CITATIONS

SEE PROFILE

Gao-Lei Hou

Pacific Northwest National Laboratory

39 PUBLICATIONS **57** CITATIONS

SEE PROFILE

Xue-Bin Wang

Pacific Northwest National Laboratory

192 PUBLICATIONS **5,263** CITATIONS

SEE PROFILE

Caroline E H Dessent

The University of York

78 PUBLICATIONS **1,489** CITATIONS

SEE PROFILE

THE JOURNAL OF PHYSICAL CHEMISTRY B

Article

pubs.acs.org/JPCB

Electron Detachment as a Probe of Intrinsic Nucleobase Dynamics in Dianion-Nucleobase Clusters: Photoelectron Spectroscopy of the Platinum II Cyanide Dianion Bound to Uracil, Thymine, Cytosine, and Adenine

Ananya Sen,[†] Gao-Lei Hou,[‡] Xue-Bin Wang,*[,‡] and Caroline E. H. Dessent*[,†]

[†]Department of Chemistry, University of York, Heslington, York YO10 5DD, U.K.

[‡]Physical Sciences Division, Pacific Northwest National Laboratory, MS K8-88, P.O. Box 999, Richland, Washington 99352, United States

Supporting Information

ABSTRACT: We report the first low-temperature photoelectron spectra of isolated gas-phase complexes of the platinum II cyanide dianion bound to nucleobases. These systems are models for understanding platinum-complex photodynamic therapies, and a knowledge of the intrinsic photodetachment properties is crucial for characterizing their broader photophysical properties. Well-resolved, distinct peaks are observed in the spectra, consistent with complexes where the $Pt(CN)_4^{2-}$ moiety is largely intact. Adiabatic electron detachment energies for the dianion-nucleobase complexes are measured to be 2.39−2.46 eV. The magnitudes of the repulsive Coulomb barriers of the complexes are estimated to be between 1.9 and 2.1 eV, values that are lower than for the bare $Pt(CN)_4^{2-}$ dianion as a result of charge solvation by the nucleobases. In addition to the resolved spectral features, broad featureless bands indicative of delayed electron detachment are observed in the 193 nm photoelectron spectra of the four dianion-nucleobase complexes and also in the 266 nm spectra of the $Pt(CN)_4^{2-}$·thymine and $Pt(CN)_4^{2-}$·adenine complexes. The selective excitation of these features in the 266 nm spectra is attributed to one-photon excitation of [$Pt(CN)_4^{2-}$·thymine]* and [$Pt(CN)_4^{2-}$·adenine]* long-lived excited states that can effectively couple to the electron detachment continuum, producing strong electron detachment signals. We attribute the delayed electron detachment bands observed here for $Pt(CN)_4^{2-}$·thymine and $Pt(CN)_4^{2-}$·adenine but not for $Pt(CN)_4^{2-}$·uracil and $Pt(CN)_4^{2-}$·cytosine to fundamental differences in the individual nucleobase photophysics following 266 nm excitation. This indicates that the $Pt(CN)_4^{2-}$ dianion in the clusters can be viewed as a "dynamic tag" which has the propensity to emit electrons when the attached nucleobase displays a long-lived excited state.

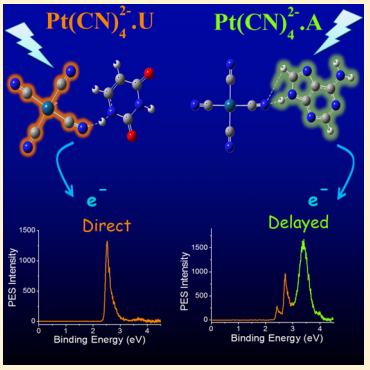

INTRODUCTION

The photophysical behavior of DNA is a subject of considerable current interest since the absorption of UV light can lead to biological damage including strand breaks and mutations.[1] A major goal of the photobiology community has therefore been to obtain an understanding of DNA photophysics on the molecular level, i.e., through an understanding of the photophysical properties of the individual nucleobases.[2] Detailed experimental and theoretical studies have revealed that all four DNA nucleobases, along with RNA base uracil, display strong UV absorptions at around 4.7 eV associated with the excitation of a $^1\pi-\pi^*$ excited state, which undergoes rapid relaxation via conical intersections back to the electronic ground state.[3,4]

In a recent study, we investigated the UV spectroscopy of isolated nucleobase-bound $Pt(CN)_4^{2-}$ complexes, i.e., Pt-$(CN)_4^{2-}$·M where M = uracil (U), thymine (T), cytosine (C), and adenine (A).[5,6] These metal-complex nucleobase clusters represent model systems for identifying the fundamental photophysical and photochemical processes occurring in photodynamic platinum(II) drug therapies that target DNA. Each of the complexes studied displays a prominent UV absorption band ($\lambda_{max} \approx 4.7$ eV) which we assigned to a nucleobase-localized chromophore and a subsequent increase in absorption intensity toward higher spectral energy assigned to $Pt(CN)_4^{2-}$ localized transitions. However, strikingly different band widths of the ∼4.7 eV band were observed across the series of complexes, with the $Pt(CN)_4^{2-}$·thymine band being more than twice the width of the $Pt(CN)_4^{2-}$·cytosine band. Intriguingly, these differences in absorption bandwidth were correlated with a dramatic change in the photochemical products observed upon excited-state decay, with the narrow-band $Pt(CN)_4^{2-}$·cytosine and $Pt(CN)_4^{2-}$·adenine complexes decaying with enhanced photofragments associated with electron detachment decay. We speculated that the enhanced electron detachment decay in the narrow-band complexes

Received: July 22, 2015
Revised: August 3, 2015

DOI: 10.1021/acs.jpcb.5b07108
J. Phys. Chem. B XXXX, XXX, XXX−XXX

resulted from relatively longer nucleobase excited-state lifetimes in these complexes, an argument that relies on the assumption that the intrinsic electron detachment properties of the series of $Pt(CN)_4^{2-}$·M complexes are the same.

In this work, we directly investigate the intrinsic electron detachment characteristics of the $Pt(CN)_4^{2-}$·M complexes by acquiring their photoelectron spectra (PES).[7,8] We aim to firmly establish the electron detachment energies of the clusters and also obtain estimates of the repulsive Coulomb barrier (RCB) heights for these multiply charged anions. These are the first measurements of dianions bound directly to a nucleobase and hence contribute crucial fundamental information on how the proximity of negative charge to a nucleobase affects the intrinsic photophysics and decay dynamics. The systems studied here are therefore relevant to understanding the UV excitation and decay process of important anionic biomolecules including nucleosides and nucleotides.[9−12]

METHODS

The PES experiments were performed with a low-temperature, magnetic-bottle time-of-flight photoelectron spectrometer coupled to an electrospray ion source (ESI) and a temperature-controllable cryogenic ion trap.[13] $Pt(CN)_4^{2-}$·M complexes were produced by electrospraying into the gas phase a 0.1 mM solution of $K_2Pt(CN)_4$ and nucleobases dissolved in mixed H_2O/CH_3OH (1/3) solvent. No experiments were conducted for the nucleobase guanine due to its low solubility in water. We note that the clusters studied in this work are expected to consist of the native keto forms of the nucleobases, as these tautomers are known to be dominate upon electrospray ionization.[14]

The anions generated were guided by quadrupole ion guides into a cryogenic ion trap. The cooling of the clusters to 20 K in the trap eliminated the possibility of the appearance of extra spectral peaks in the PES spectra due to hot bands. These anion clusters were then mass-selected and decelerated before being photodetached by an Nd:YAG laser (266 nm, 4.661 eV) or an ArF laser (193 nm, 6.424 eV) in the photodetachment zone of the magnetic-bottle, photoelectron analyzer. The laser was operated at a 20 Hz repetition rate with the ion beam off at alternating laser shots to enable shot-to-shot background subtraction to be carried out. Photoelectrons were collected at ∼100% efficiency with an energy resolution of 20 meV for electrons with 1 eV of kinetic energy.

RESULTS

Photoelectron spectra of the $Pt(CN)_4^{2-}$·M complexes were obtained at both 266 and 193 nm. Figure 1 displays the 266 nm spectra of the complexes, which are each characterized by a first band that peaks in the 2.5 eV binding-energy region. The photoelectron spectroscopy of the bare $Pt(CN)_4^{2-}$ dianion has been studied in detail in previous work by one of our groups,[15] and the 266 nm spectrum of the $Pt(CN)_4^{2-}$ dianion similarly displays a prominent band at around 1.7 eV resulting from partially resolved X and A bands. We assign the 2.5 eV bands observed here for the $Pt(CN)_4^{2-}$·M complexes to the analogous X/A band. Two distinctive bands are evident in this region (2.4−2.8 eV binding energy) of the spectra for $Pt(CN)_4^{2-}$·C and $Pt(CN)_4^{2-}$·A (Figure 1c,d). We assign these bands to the X/A features associated with the presence of two cluster isomers (I and II) for these complexes, as illustrated in Figure 1c,d. Ab initio calculations have revealed the existence of

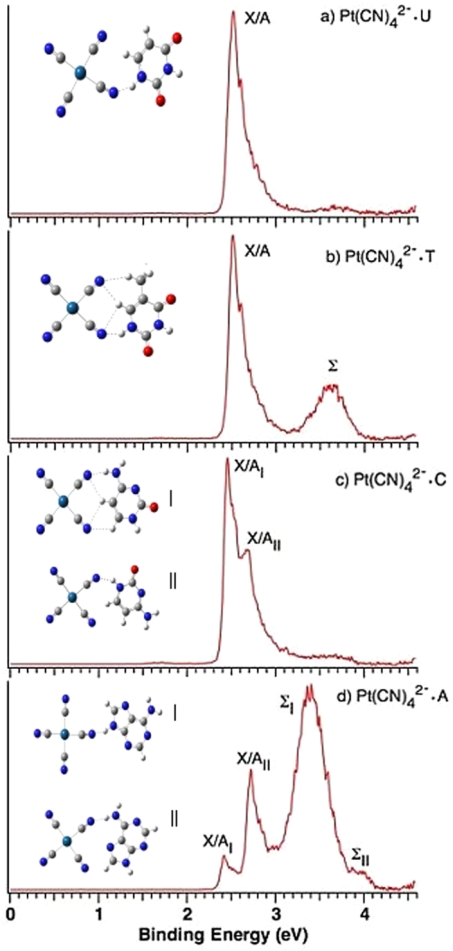

Figure 1. Photoelectron spectra of (a) $Pt(CN)_4^{2-}$·U, (b) $Pt(CN)_4^{2-}$·T, (c) $Pt(CN)_4^{2-}$·C, and (d) $Pt(CN)_4^{2-}$·A obtained at 266 nm. Schematic illustrations of the global minimum structures of the complexes are included,[16] illustrating the two isomeric structures that contribute to the $Pt(CN)_4^{2-}$·C and $Pt(CN)_4^{2-}$·A spectra.

two low-energy cluster isomers for each of the $Pt(CN)_4^{2-}$·M complexes,[16] associated with the relative arrangement of the nucleobase with $Pt(CN)_4^{2-}$. (The tautomeric form of the nucleobase is the keto form in both isomers I and II since this is the nucleobase tautomer we expect to obtain upon electrospray ionization.[14]) However, the relative energies of isomers I and II are much closer for $Pt(CN)_4^{2-}$·C and $Pt(CN)_4^{2-}$·A (ΔE = 0.25 and 0.51 eV, respectively) than for $Pt(CN)_4^{2-}$·U and $Pt(CN)_4^{2-}$·T (ΔE = 0.94 and 0.96 eV, respectively). Variable-temperature PES (20 and 300 K) were recorded for $Pt(CN)_4^{2-}$·A and are included in the SI (Figure S1). There is some loss in spectral resolution with the increase in temperature from 20 to 300 K, but the same number of spectral features and hence the same number of isomers appear to be present at the two temperatures. This indicates that the barriers for interconverting the cluster isomers are considerable, presumably due to the presence of the strong ionic hydrogen bonds and the substantial geometric differences between the respective pairs of isomers (insets in Figure 1c,d).[16]

The differences in energy between the vertical detachment energies (VDEs) of the X/A_I band in bare $Pt(CN)_4^{2-}$ and the complexes, Δ_{VDE} (Table 1), represent the differential binding energies of the complexes on the ground-state dianionic surfaces compared to those on the monoanionic (electron-

DOI: 10.1021/acs.jpcb.5b07108
J. Phys. Chem. B XXXX, XXX, XXX−XXX

Table 1. Adiabatic Detachment Energy (ADE), Vertical Detachment Energy (VDE) and Δ_{VDE} Values for the X Band of the $Pt(CN)_4^{2-}$ Dianion and $Pt(CN)_4^{2-}$·M Complexes Obtained from the 266 nm PES Spectra (in eV)[a]

	ADE[b]	X/A_I (VDE)[c]	X/A_{II} (VDE)[c]	Δ_{VDE}[d]	Σ
$Pt(CN)_4^{2-}$	1.69[e]	1.69[e]			
$Pt(CN)_4^{2-}$·U	2.44(3)	2.52 (1)		0.83	
$Pt(CN)_4^{2-}$·T	2.46(3)	2.51(1)		0.82	3.6
$Pt(CN)_4^{2-}$·C	2.42(3)	2.46 (1)	2.67 (2)	0.77	
$Pt(CN)_4^{2-}$·A	2.39(3), 2.67(3)[f]	2.42 (1)	2.72 (1)	0.73	3.4

[a]Numbers in parentheses represent experimental uncertainties in the last digits. [b]ADE was obtained by adding the instrumental resolution to the electron binding energy at the crossing point of the onset of the spectral feature and the baseline. [c]The VDEs were measured from the respective spectral band maxima. [d]The Δ_{VDE} values are the shift in the VDE (X/A_I band) of the complex relative to uncomplexed $Pt(CN)_4^{2-}$. [e]From ref 15. [f]Estimate for isomer II.

detached) surfaces. We anticipate that Δ_{VDE} should provide a measure of the dianion-nucleobase binding energy, since no significant geometric rearrangement would be expected upon electron detachment. The Δ_{VDE} values indicate that the binding energy decreases along the series $Pt(CN)_4^{2-}$·U > ≈ $Pt(CN)_4^{2-}$·T > $Pt(CN)_4^{2-}$·C > $Pt(CN)_4^{2-}$·A, a trend that mirrors the previously calculated binding energies for the dianionic complexes (1.75, 1.69, 1.55, and 1.45 eV, respectively).[16]

In addition to the X/A bands, the 266 nm PES of $Pt(CN)_4^{2-}$·T and $Pt(CN)_4^{2-}$·A both display broad resonance features centered at 3.6 and 3.4 eV, respectively, labeled Σ on Figure 1b,d. (A Σ feature for isomer II is also evident in the $Pt(CN)_4^{2-}$·A spectrum with reduced intensity due to the RCB cutoff, vide infra.) Similar but much lower intensity features are also visible at ∼3.7 eV in both the $Pt(CN)_4^{2-}$·U and $Pt(CN)_4^{2-}$·C spectra. The origin of these features will be discussed below. Table 1 lists the adiabatic and vertical detachment energies (ADEs and VDEs), along with the Δ_{VDE} values for the $Pt(CN)_4^{2-}$·M clusters.

Figure 2 displays the 193 nm PES spectra of the $Pt(CN)_4^{2-}$·M complexes, along with a 193 nm PES spectrum for the bare $Pt(CN)_4^{2-}$ dianion which we reacquired for this study. The previous 193 nm PES study of bare $Pt(CN)_4^{2-}$ identified nine resolved spectral features (X, A–H), and these are labeled on the spectrum displayed in Figure 2a, where they appear as resolved features. The greater number of bands observed with 193 nm photodetachment compared to the number at 266 nm is a result of the higher photon energy being sufficient to exceed the RCB for the higher-lying states. The 193 nm spectra of the $Pt(CN)_4^{2-}$·M complexes (Figure 2b–e) provide ADEs in excellent agreement with those obtained at 266 nm (Table 1) for all of the complexes. The 193 nm VDE (X/A_I) for $Pt(CN)_4^{2-}$·A also agrees well with the value obtained at 266 nm; however, the VDE values of the X/A_I bands for M = U, T, and C and the VDEs of the X/A_{II} bands for M = C and A measured from the 193 nm spectra (Table 2) are larger by 0.06–0.09 eV than those obtained from the respective 266 nm spectra (Table 1). This is a result of tunnelling modulation of the X/A bands, which occurs when the 266 nm photon energy is in the vicinity of the tops of the respective RCB curves.[7,8]

We now turn to the assignment of the A–G electronic bands for the $Pt(CN)_4^{2-}$·M clusters. Considering the $Pt(CN)_4^{2-}$·U spectrum (Figure 2b) first, sharp peaks B–D can be clearly identified in the spectrum at binding energies above the X/A

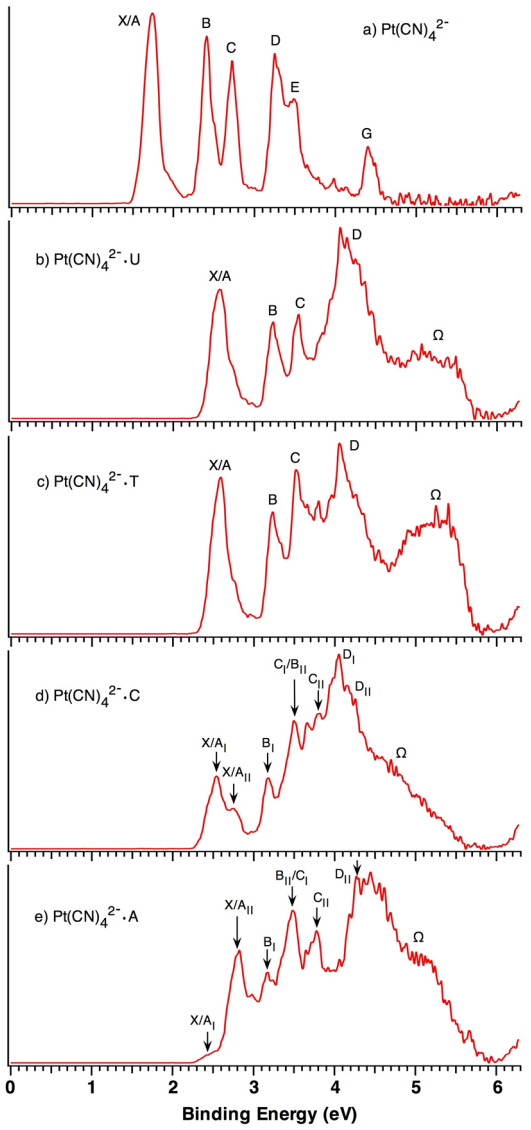

Figure 2. Photoelectron spectra of (a) the bare $Pt(CN)_4^{2-}$ dianion, (b) $Pt(CN)_4^{2-}$·U, (c) $Pt(CN)_4^{2-}$·T, (d) $Pt(CN)_4^{2-}$·C, and (e) $Pt(CN)_4^{2-}$·A obtained at 193 nm.

feature. This indicates that the $Pt(CN)_4^{2-}$ moiety is largely intact within the cluster. Each band, like the X/A band, is shifted to a higher binding energy by 0.8 eV compared to the corresponding feature in the $Pt(CN)_4^{2-}$ spectrum. However, it is evident that the $Pt(CN)_4^{2-}$·U spectrum also contains a broad featureless band contributing to the overall electron signal between ∼3.0 and 5.0 eV so that the sharp B–D features reside on top of this band. The presence of the enhanced electron detachment signal in the high-binding region of the spectrum results in the D band in particular appearing relatively more intense than the X/A band compared to the $Pt(CN)_4^{2-}$ spectrum (Figure 2a). We note that the D band assigned in this work corresponds to unresolved D–F bands identified in the previous study of uncomplexed $Pt(CN)_4^{2-}$.[15] A similar pattern is evident for $Pt(CN)_4^{2-}$·T (Figure 2c), with the spectrum corresponding to sharp $Pt(CN)_4^{2-}$-centered features (X/A–D), combined with a featureless enhanced electron signal between 3.0 and 5.0 eV. As in the 266 nm spectra, the $Pt(CN)_4^{2-}$·C and $Pt(CN)_4^{2-}$·A 193 nm spectra again contain contributions from the two cluster isomers (I and II), and each

DOI: 10.1021/acs.jpcb.5b07108
J. Phys. Chem. B XXXX, XXX, XXX–XXX

Table 2. Vertical Detachment Energies (VDE) of the Features Observed in the PES Spectra of the $Pt(CN)_4^{2-}$ Dianion and $Pt(CN)_4^{2-}$·M Complexes Obtained at 193 nm, along with the Estimated Repulsive Coulomb Barriers (RCB)[a,b]

	X/A_I[c]	X/A_{II}[c]	B_I	B_{II}	C_I	C_{II}	D_I	D_{II}	RCB
$Pt(CN)_4^{2-}$	1.74		2.41		2.72		3.25		~2.5[d]
$Pt(CN)_4^{2-}$·U	2.58		3.23		3.54		4.06		~2.1
$Pt(CN)_4^{2-}$·T	2.59		3.23		3.52		4.06		~2.1
$Pt(CN)_4^{2-}$·C	2.54	2.75	3.18	3.50	3.50	3.80	4.05	~4.2	~2.1
$Pt(CN)_4^{2-}$·A	2.42	2.81	3.18	3.48	3.48	3.78		4.28	~1.9

[a]All values are in eV. [b]All values are vertical detachment energies (peaks of bands) with experimental uncertainties of ±0.03 eV. [c]The VDEs for X/A_I bands of the $Pt(CN)_4^{2-}$U/T/C complexes and the VDE for the X/A_{II} band for the $Pt(CN)_4^{2-}$·A complex are slightly larger by 0.06 to 0.09 eV than those respective values estimated from the 266 nm spectra (Table 1). This is due to the existence of RCBs, which results in a slight red shift in energy for the X/A bands at 266 nm, from which the magnitudes of RCBs are estimated. [d]Reference 15.

spectrum can be assigned by assuming the presence of bands X/A−D for each isomer. (Figures S2, S3 of the SI provides simulated spectra to support this assignment.) Featureless enhanced electron signals again appear to contribute to the spectra between ~3.0 and 5.0 eV. We use symbol Ω to label the 3.0−5.0 eV featureless bands that contribute to each of the 193 nm spectra. Simulations of each of these $Pt(CN)_4^{2-}$·M spectra are included in the SI (Figures S2−S5). These simulations illustrate that the profiles of the experimental spectra (Figure 2b−e) can be reproduced by combining the contributions from a broad featureless electron detachment band (Ω) with the direct detachment features associated with detachment from the $Pt(CN)_4^{2-}$ moiety within the clusters. (It is notable that the 193 nm photodetachment of isolated $Pt(CN)_4^{2-}$ does not result in a broad detachment feature since the photoelectron spectrum displays only sharp spectral peaks.[15] Therefore, the Ω features arise due to the presence of the nucleobases.)

Approximate values for the RCB heights of the $Pt(CN)_4^{2-}$·M complexes can be determined by comparing the electronic X/A features present in spectra in Figures 1 and 2. The fact that VDEs of the X/A_I bands for the U, T, and C complexes and VDEs of the X/A_{II} bands of the C and A clusters obtained at 266 nm are slightly smaller than those corresponding values measured at 193 nm suggests that the 266 nm photon energy is just around the top of the respective RCB curves for the X/A channels, resulting in tunnelling modulation for the appearance of the X/A bands at 266 nm,[7,8] from which the RCB heights were estimated (Table 2). All of the $Pt(CN)_4^{2-}$·M RCB values (Table 2) are lower than the value for the $Pt(CN)_4^{2-}$ dianion (~2.5 eV),[15] in line with the expected reduction in the RCB due to charge solvation by the nucleobase moiety.[7,17,18] The RCB values of ~2.1 eV for the U, T, and C metal complexes and ~1.9 eV for the A complex are also in accordance with the lengths of the intermolecular bonds in the four nucleobase complexes.

DISCUSSION

The Σ and Ω features which are observed in the 266 and 193 nm spectra presented above cannot be straightforwardly assigned to spectral features related to the photodetachment of the $Pt(CN)_4^{2-}$ moiety within the clusters: the Σ and Ω features are not associated with the A−H electronic states of the photodetached dianion. In considering the origin of the Σ and Ω features, it is first crucially important to note that the Σ features are observed for only two of the four complexes studied at 266 nm, i.e., for $Pt(CN)_4^{2-}$·T and $Pt(CN)_4^{2-}$·A. The fact that these Σ features are not present for all of the clusters allows us to rule out a number of possibilities. For example, we can immediately rule out the possibility that these features arise from the photodetachment of anionic fragments produced by initial photoexcitation of the cluster. Photoexcitation of each of the four $Pt(CN)_4^{2-}$·M clusters results in the production of numerous photofragments, but there is no reason why photoelectron signals from these fragments would only be observed for two of the four complexes upon 266 nm excitation. Moreover, if such fragments did produce photoelectron bands they would not be broad and featureless. As an example, the $Pt(CN)_4^{2-}$ dianion is a known photofragment for each of these clusters, and it is clear that there is no spectral signature of this dianion (ADE = 1.7 eV) in the spectra of the parent clusters (Figures 1 and 2). A second possibility is that the Σ and Ω features arise from the photodetachment of the $Pt(CN)_4^{-}$·M monoanion after initial photodetachment of the doubly charged anion. This is highly unlikely, as the Σ signal is too strong to be assigned to such a two-photon process, in particular for $Pt(CN)_4^{2-}$·A. Furthermore, given that the ADEs and RCBs for all four $Pt(CN)_4^{2-}$·M complexes are similar, the ADEs for the $Pt(CN)_4^{-}$·M monoanions should also be similar. Therefore, if this type of two-photon mechanism were correct, then Σ features should have been seen in the 266 nm spectra of the four $Pt(CN)_4^{2-}$·M complexes. These considerations lead us to consider nucleobase-dependent mechanisms for the Σ features.

The dominant Σ bands observed in the 266 nm spectra of $Pt(CN)_4^{2-}$·T and $Pt(CN)_4^{2-}$·A and the Ω bands seen in the 193 nm spectra (Figures S2−S5 of the SI) are broad and unstructured and therefore typical of bands that arise following "resonant" or "delayed" electron emission. Such electron detachment can arise from the decay of a $[Pt(CN)_4^{2-}·M]^*$ excited state which is accessed in a single photon transition and subsequently decays by electron emission, rather than the typical (instantaneous) direct detachment process. Such features have been observed previously in photoelectron spectroscopy studies[19−21] and in particular in a study by Matheis et al. of doubly deprotonated gramicidin polypeptide polyanions.[19] In that work, the authors presented their photoelectron spectra both as a function of electron binding energy and also as a function of electron kinetic energy to illustrate that the resonant detachment features display bands at the same electron kinetic energies for different photon energies, which is strongly indicative of delayed emission.[20,21] Similar spectra (presented versus electron kinetic energy) are presented in the SI material (Figures S6 and S7) for the $Pt(CN)_4^{2-}$·M complexes studied here, providing strong support for the assignment of the Σ and Ω features as arising from delayed emission following resonant excitation of the clusters, by direct analogy with the results of Matheis et al.[19]

DOI: 10.1021/acs.jpcb.5b07108
J. Phys. Chem. B XXXX, XXX, XXX−XXX

The cut-offs in the low electron kinetic energy region of the plots displayed in the SI (Figures S6 and S7) provide values for the RCBs of the excited states accessed in the resonant detachment process. These RCBs have values of between ~0.8−1.0 eV and are therefore considerably smaller than the RCBs associated with direct detachment from the $Pt(CN)_4^{2-}$ moiety within the $Pt(CN)_4^{2-}$·M clusters (~1.9−2.1 eV, Table 1). The fact that these RCBs can be observed and that they display distinctive values from those for direct detachment provide further support for the assignment of the broad Σ and Ω features as arising from resonant detachment from the dianionic complexes.

In deprotonated gramicidin, Matheis et al. have suggested that delayed electron emission may occur after resonant photoexcitation either from a long-lived excited state that couples to the ionization continuum via electron tunnelling emission or after internal conversion leading to emission from the hot ground state.[19] From our previous CID studies of the $Pt(CN)_4^{2-}$·M ground-state complexes, we know that the (thermally excited) ground-state complexes show no propensity to decay via electron emission.[16] Therefore, it seems that in the clusters studied here, one-photon excitation accesses long-lived $[Pt(CN)_4^{2-}·M]^*$ excited states which can selectively couple to the electron detachment continuum, producing strong electron emission signals. At the higher 193 nm photon energy (6.424 eV), all of the clusters display a significant propensity to produce delayed emission signals. This is consistent with the previous UV laser photodissociation spectroscopy of these clusters. All of the clusters displayed significant absorption cross sections above 5.6 eV,[5,6] which correlates with the production of electron detachment photofragments, in line with the delayed emission observed here.

The differences between the 266 nm $Pt(CN)_4^{2-}$·M photoelectron spectra in terms of the dominance of the delayed detachment features (Σ) is striking, where 266 nm excitation appears to access long-lived excited states for $[Pt(CN)_4^{2-}·T]^*$ and $[Pt(CN)_4^{2-}·A]^*$ that effectively couple to the electron detachment continuum. This appears to contrast with the situation for the $Pt(CN)_4^{2-}$·U and $Pt(CN)_4^{2-}$·C complexes, where any similar excited states accessed at this wavelength are not sufficiently long-lived to effectively couple to the electron detachment continuum. The photoexcitation of isolated nucleobases has been intensively studied both experimentally and theoretically for wavelengths close to 266 nm.[3,4,22−24] The excited-state decay dynamics of individual nucleobases change dramatically as a function of photoexcitation wavelength since the region of the excited-state potential surface accessed will determine the proximity to conical intersections which facilitate ultrafast decay. In this context, the substantial delayed emission bands observed here for $Pt(CN)_4^{2-}$·T and $Pt(CN)_4^{2-}$·A but not for $Pt(CN)_4^{2-}$·U and $Pt(CN)_4^{2-}$·C can be traced to fundamental differences in the individual nucleobase photophysics rather than to differences due to properties of the aggregated cluster.

FURTHER DISCUSSION

The overall picture to emerge from the PES of the $Pt(CN)_4^{2-}$·M clusters is that each of the clusters displays similar fundamental electron detachment properties: the complexes have very similar electron detachment energies as well as similar RCBs, and the spectra are all consistent with clusters where the $Pt(CN)_4^{2-}$ dianion is largely unperturbed by the adjacent nucleobase. These similarities continue in the 193 nm spectra, with respect to the appearance of delayed electron detachment features that are evident for each of the four complexes. As discussed above, we concluded that this delayed detachment results from the initial excitation of a nucleobase-centered chromophore. Although nucleobase excited-state dynamics have been intensively studied, little is known about excitation and decay mechanisms in this far-UV spectral region. In the lower-energy near- and mid-UV ranges, native nucleobases are frequently viewed as being "designed" or "selected" so that the primary excited states accessed will undergo ultrafast decay, hence minimizing the possibility of radiation-induced damage.[25] However, since biological systems are not exposed to far-UV excitation, there is no requirement for the nucleobases to undergo ultrafast decay following excitation in this spectral region.

It is evident that the same electronic excited state is being accessed in the photoexcitation of the $Pt(CN)_4^{2-}$·M clusters at both 266 and 193 nm since the observed RCBs in the electron kinetic energy plots (Figures S6 and S7 of the SI) are identical. However, the region of the excited-state potential energy surface accessed is clearly different at the two excitation wavelengths. From state-of-the-art ab initio simulations, it is well known that the possible decay channels and deactivation time constants for a photoexcited nucleobase vary critically with excitation energy, particularly in the region around 266 nm.[4,22−24,26] In this context, it is unsurprising that the delayed emission features associated with the presence of longer-lifetime components are nucleobase-dependent. Such nucleobase-dependent photophysics in dianion-nucleobase clusters was also observed in our previous electronic spectroscopy studies of the $Pt(CN)_4^{2-}$·M clusters, where the photophysical and photochemical properties were studied for photoexcitation energies between ~4.1 and 5.7 eV.[5] From the photoelectron spectra acquired in the current work, it is now clear that the electronic spectra were all recorded just above the electron detachment thresholds of the clusters. However, the propensity for the excited-state clusters to decay via electron emission was both wavelength- and nucleobase-dependent.

CONCLUSIONS AND PERSPECTIVES

Low-temperature photoelectron spectra have been recorded for the $Pt(CN)_4^{2-}$·M (M = U, T, C, and A) complexes. The spectra are consistent with complexes where the $Pt(CN)_4^{2-}$ moiety is largely intact, and the complexes all display similar adiabatic electron detachment energies and repulsive Coulomb barriers. In addition to direct electron detachment features associated with electron detachment from the $Pt(CN)_4^{2-}$ dianion, the spectra also display broad unstructured features which we attribute to delayed electron emission following resonant excitation of nucleobase-centered chromophores on the clusters. While significant delayed emission is observed for all four complexes at 193 nm, the extent of delayed emission is dramatically different for the four complexes at 266 nm. This suggests the intriguing possibility that the $Pt(CN)_4^{2-}$ dianion in the $Pt(CN)_4^{2-}$·M clusters can therefore be viewed as a "dynamic tag" which has the propensity to emit electrons when nucleobase decay occurs over longer time scales. From the measurements made in this work, it is not possible to give any estimates of the time scales involved, but future time-resolved dynamical measurements of the $Pt(CN)_4^{2-}$·M clusters are warranted to provide a more detailed picture of these key dynamical processes.[27]

DOI: 10.1021/acs.jpcb.5b07108
J. Phys. Chem. B XXXX, XXX, XXX−XXX

■ ASSOCIATED CONTENT

Supporting Information

The Supporting Information is available free of charge on the ACS Publications website at DOI: 10.1021/acs.jpcb.5b07108.

Photoelectron spectra of $Pt(CN)_4^{2-}$·A obtained at 193 nm. Simulated 193 nm photoelectron spectra for $Pt(CN)_4^{2-}$·C, $Pt(CN)_4^{2-}$·A, $Pt(CN)_4^{2-}$·U, and $Pt(CN)_4^{2-}$·T. Photoelectron spectra for $Pt(CN)_4^{2-}$·C, $Pt(CN)_4^{2-}$·A, $Pt(CN)_4^{2-}$·U, and $Pt(CN)_4^{2-}$·T vs electron kinetic energy to illustrate the presence of delayed electron emission. A description of how the simulated spectra were produced. (PDF)

■ AUTHOR INFORMATION

Corresponding Authors

*E-mail: xuebin.wang@pnnl.gov. Fax: 01-509-371-6139.
*E-mail: caroline.dessent@york.ac.uk. Fax: 44-1904-322516.

Notes

The authors declare no competing financial interest.

■ ACKNOWLEDGMENTS

This work was supported through European Research Council grant 208589-BIOIONS. A.S. acknowledges a Pacific Northwest National Laboratory Alternate Sponsored Fellowship. Photoelectron spectra work at PNNL was supported by the U.S. Department of Energy (DOE), Office of Science, Office of Basic Energy Sciences, Division of Chemical Sciences, Geosciences and Biosciences, and was performed at the EMSL, a national scientific user facility sponsored by DOE's Office of Biological and Environmental Research and located at Pacific Northwest National Laboratory, which is a multiprogram national laboratory operated for DOE by Battelle Memorial Institute.

■ REFERENCES

(1) Boudaiffa, B.; Cloutier, P.; Hunting, D.; Huels, M. A.; Sanche, L. Resonant Formation of DNA Strand Breaks by Low-Energy (3 to 20 eV) Electrons. *Science* **2000**, *287*, 1658−1660.

(2) Middleton, C. T.; de La Harpe, K.; Su, C.; Law, Y. K.; Crespo-Hernández, C. E.; Kohler, B. DNA Excited-State Dynamics: From Single Bases to the Double Helix. *Annu. Rev. Phys. Chem.* **2009**, *60*, 217−239.

(3) Kleinermanns, K.; Nachtigallova, D.; de Vries, M. S. Excited State Dynamics of DNA Bases. *Int. Rev. Phys. Chem.* **2013**, *32*, 308−342.

(4) Barbatti, M.; Aquino, A. J. A.; Szymczak, J. J.; Nachtigallova, D.; Hobza, P.; Lishchka, H. Relaxation Mechanisms of UV-Photoexcited DNA and RNA Nucleobases. *Proc. Natl. Acad. Sci. U. S. A.* **2010**, *107*, 21453−21458.

(5) Sen, A.; Dessent, C. E. H. Photoactivation of Nucleobase Bound Platinum II Metal Complexes: Probing the Influence of the Nucleobase. *J. Chem. Phys.* **2014**, *141*, 241101−241105.

(6) Sen, A.; Dessent, C. E. H. Mapping the UV Photophysics of Platinum Metal Complexes Bound to Nucleobases: Laser Spectroscopy of Isolated Uracil·$Pt(CN)_4^{2-}$ and Uracil·$Pt(CN)_6^{2-}$ Complexes. *J. Phys. Chem. Lett.* **2014**, *5*, 3281−3285.

(7) Wang, L. S.; Wang, X. B. Probing Free Multiply Charged Anions Using Photodetachment Photoelectron Spectroscopy. *J. Phys. Chem. A* **2000**, *104*, 1978−1990.

(8) Wang, X. B.; Ding, C. F.; Wang, L. S. Photodetachment Spectroscopy of a Doubly Charged Anion: Direct Observation of the Repulsive Coulomb Barrier. *Phys. Rev. Lett.* **1998**, *81*, 3351−3354.

(9) Chatterley, A. S.; West, C. W.; Roberts, G. M.; Stavros, V. G.; Verlet, J. R. R. Mapping the Ultrafast Dynamics of Adenine Onto its Nucleotide and Oligonucleotides by Time-Resolved Photoelectron Imaging. *J. Phys. Chem. Lett.* **2014**, *5*, 843−848.

(10) Weber, J. M.; Ioffe, I. N.; Berndt, K. M.; Löffler, D.; Friedrich, J.; Ehrler, O. T.; Danell, A. S.; Parks, J. H.; Kappes, M. M. Photoelectron Spectroscopy of Isolated Multiply Negatively Charged Oligonucleotides. *J. Am. Chem. Soc.* **2004**, *126*, 8585−8589.

(11) Nielsen, S. B.; Andersen, J. U.; Forster, J. S.; Hvelplund, P.; Liu, B.; Pedersen, U. V.; Tomita, S. Photodestruction of Adenosine 5′-Monophosphate (AMP) Nucleotide Ions In Vacuo. Statistical Versus Non-Statistical Processes. *Phys. Rev. Lett.* **2003**, *91*, 048302.

(12) Brondsted Nielsen, S.; Sølling, T. I. Are Conical Intersections Responsible for the Ultrafast Processes of Adenine, Protonated Adenine and the Corresponding Nucleosides? *ChemPhysChem* **2005**, *6*, 1276−1281.

(13) Wang, X. B.; Wang, L. S. Development of a Low-Temperature Photoelectron Spectroscopy Instrument Using an Electrospray Ion Source and a Cryogenically Controlled Ion Trap. *Rev. Sci. Instrum.* **2008**, *79*, 0731081−8.

(14) *Nucleic Acids in the Gas Phase*; Gabelica,V., Ed.; Springer, 2014; Chapter 1.

(15) Wang, X. B.; Wang, Y. L.; Woo, H. K.; Li, J.; Wu, G. S.; Wang, L. S. Free Tetra- and Hexa-Coordinated Platinum-Cyanide Dianions, $Pt(CN)_4^{2-}$ and $Pt(CN)_6^{2-}$. A Combined Photodetachment Photoelectron Spectroscopic and Theoretical Study. *Chem. Phys.* **2006**, *329*, 230−238.

(16) Sen, A.; Luxford, T. F. M.; Yoshikawa, N.; Dessent, C. E. H. Solvent Evaporation Versus Proton Transfer in Nucleobase-Pt-$(CN)_{4,6}^{2-}$ Dianion Clusters: A Collisional Excitation and Electronic Laser Photodissociation Spectroscopy Study. *Phys. Chem. Chem. Phys.* **2014**, *16*, 15490−15500.

(17) Boxford, W. E.; Dessent, C. E. H. On the Stability of $IrCl_6^{3-}$ and Other Triply Charged Anions: Solvent Stabilization Versus Ionic Fragmentation and Electron Detachment for the $IrCl_6^{3-}\cdot(H_2O)_n$ n = 0−10 Microsolvated Clusters. *J. Phys. Chem. A* **2005**, *109*, 5836−5845.

(18) Boxford, W. E.; Dessent, C. E. H. Probing the Intrinsic Features and Environmental Stabilization of Multiply Charged Anions. *Phys. Chem. Chem. Phys.* **2006**, *8*, 5151−5165.

(19) Matheis, K.; Joly, L.; Antoine, R.; Lepine, F.; Bordas, C.; Ehrler, O. T.; Allouche, A. R.; Kappes, M. M.; Dugourd, P. Photoelectron Spectroscopy of Gramicidin Polyanions: Competition Between Delayed and Direct Emission. *J. Am. Chem. Soc.* **2008**, *130*, 15903−15906.

(20) Lepine, F.; Bordas, C. Time-Dependent Spectrum of Thermionic Emission from Hot Clusters: Model and Example of C-60. *Phys. Rev. A: At., Mol., Opt. Phys.* **2004**, *69*, 053201.

(21) Campbell, E. E. B.; Levine, R. D. Delayed Ionization and Fragmentation En Route to Thermionic Emission: Statistics and Dynamics. *Annu. Rev. Phys. Chem.* **2000**, *51*, 65−98.

(22) Ullrich, S.; Schultz, T.; Zgierski, M. Z.; Stolow, A. Electronic Relaxation Dynamics in DNA and RNA Bases Studied by Time-Resolved Photoelectron Spectroscopy. *Phys. Chem. Chem. Phys.* **2004**, *6*, 2796−2801.

(23) Crespo-Hernández, C. E.; Cohen, B.; Hare, P. M.; Kohler, B. Ultrafast Excited-State Dynamics in Nucleic Acids. *Chem. Rev.* **2004**, *104*, 1977−2019.

(24) Shukla, M. K.; Leszczynski, J. Electronic Spectra, Excited State Structures and Interactions of Nucleic Acid Bases and Base Assemblies: A Review. *J. Biomol. Struct. Dyn.* **2007**, *25*, 93−118.

(25) Sagan, C. Ultraviolet Selection Pressure on the Earliest Organisms. *J. Theor. Biol.* **1973**, *39*, 195−200.

(26) Bisgaard, C. Z.; Satzger, H.; Ullrich, S.; Stolow, A. Excited State Dynamics of Isolated DNA Bases: A Case Study of Adenine. *ChemPhysChem* **2009**, *10*, 101−110.

(27) Verlet, J. R. R.; Horke, D. A.; Chatterly, A. S. Excited States of Multiply-Charged Anions Probed by Photoelectron Imaging: Riding the Repulsive Coulomb Barrier. *Phys. Chem. Chem. Phys.* **2014**, *16*, 15043−15052.

DOI: 10.1021/acs.jpcb.5b07108
J. Phys. Chem. B XXXX, XXX, XXX−XXX